УДК 537.226.4:535

V. G. Chigrinov[1], A. K. Srivastava[1], E. P. Pozhidaev[1,2]

FERROELECTRIC LIQUID CRYSTALS: PHYSICS AND APPLICATIONS

[1]State Key Lab on Advanced Displays and Optoelectronics,
Hong Kong University of Science and Technology,
Clear Water Bay, Kowloon, Hong Kong.
E-mail: eechigr@ust.hk
[2]P. N. Lebedev Physical Institute of the Russian Academy of Sciences,
53 Leninskiy Ave, Moscow, 119991, Russia.
E-mail: epozhidaev@mail.ru

Basic electro-optical effects in ferroelectric liquid crystals are considered in terms of their physical nature and potential applications in display and photonic devices of a new generation.

***Key words**: ferroelectric liquid crystals, spontaneous polarization, electro-optical effects, electrically controlled birefringence.*

DOI: 10.18083/LCAppl.2016.1.9

В. Г. Чигринов[1], А. К. Шривастава[1], Е. П. Пожидаев[1,2]

СЕГНЕТОЭЛЕКТРИЧЕСКИЕ ЖИДКИЕ КРИСТАЛЛЫ: ФИЗИКА И ОБЛАСТИ ПРИМЕНЕНИЯ

[1]Государственная лаборатория современных дисплеев и оптоэлектроники,
Гонконгский университет науки и технологии,
Залив Чистой Воды, Коулун, Гонконг.
E-mail: eechigr@ust.hk
[2]Физический институт им. П. Н. Лебедева РАН,
Ленинский пр., д. 53, 119991 Москва, Россия.
E-mail: epozhidaev@mail.ru

Основные электрооптические эффекты в сегнетоэлектрических жидких кристаллах рассмотрены с точки зрения их физической сущности и потенциала использования в дисплейных и фотонных устройствах нового поколения.

***Ключевые слова**: сегнетоэлектрические жидкие кристаллы, спонтанная поляризация, электрооптические эффекты, электроуправляемое двулучепреломление.*

1. Introduction

Five electrooptic modes in ferroelectric liquid crystals (FLC), Clark–Lagerwall mode is Surface Stabilized FLC (SSFLC) structure, Bi and Multistable FLC switching, Deformed Helix Ferroelectric (DHF), Electrically Suppressed Helix (ESH) mode, and FLC orientational electro-optic Kerr effect were proposed for fast FLCD. The very promising possibility to obtain a high contrast ratio and uniform FLC cell is to use the optimal anchoring energy, which is easy to get by using a photoalignment technology.

2. Clark-Lagerwall Effect

Let us consider the main electrooptical phenomena in FLC. The best known is the Clark–Lagerwall effect [1], which results in director reorientation from one bistable state to the other when an external electric field changes its sign (Fig. 1). In this case, the FLC layers are perpendicular to the substrates and the director moves along the surface of a cone whose axis is normal to the layers and parallel to the cell substrates. In each final position of its deviation the director remains parallel to the substrates, thus transforming the FLC cell into a uniaxial phase plate. The origin of electrooptical switching in the FLC cell is the interaction of the polarization **P** perpendicular to the director with the electric field **E**. The maximum variation of the transmitted intensity is achieved when the FLC cell is placed between crossed polarizers, so that an axis of the input polarizer coincides with one of the final director positions. The total angle of switching equals the double tilt angle θ (Fig. 1). The Clark–Lagerwall effect is observed in the so-called Surface Stabilized FLC structures (SSFLC). In SSFLC cells d << Ro and we come to the situation where the existence of the helix is unfavorable, i.e., the helix is unwound by the walls.

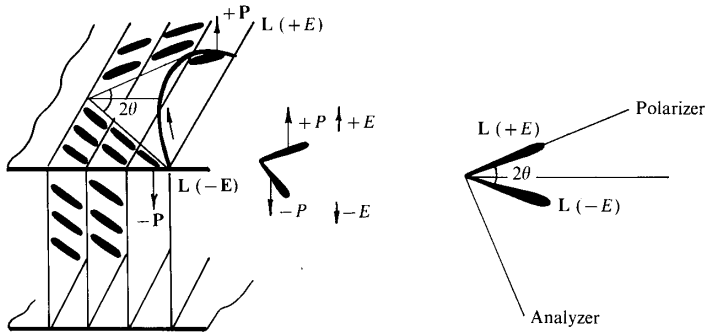

Fig. 1. Clark-Lagerwall effect in FLC cell

The response times in the Clark–Lagerwall effect are determined by $\tau_\varphi \propto \gamma_\varphi/PE$, where γ_φ is FLC rotational viscosity, P-FLC spontaneous polarization, and E-applied electric field (Fig.1) [1, 2]. Comparing the response times in nematics (N):

$$\tau_r^{(N)} \propto 4\pi\gamma_1/\Delta\varepsilon E^{2,} \quad \tau_d^{(N)} \propto d^2\gamma_1/K\pi^2 , \qquad (1)$$

where K – in nematic LC elastic constant, γ_1 – rotational viscosity, d – thickness of the layer, and ferroelectric liquid crystals (FLC)

$$\tau_r^{(FLC)} \propto \tau_d^{(FLC)} \propto \tau_\varphi \propto \gamma_\varphi/PE, \qquad (2)$$

we come to conclusion that the electrooptical switching in the Clark–Lagerwall effect in FLCs is much faster than in nematic LC. Slower response of nematic LCs is mainly due to the relatively large decay times $\tau_d^{(N)}$, which in FLC case can be very short in sufficiently high electric fields E.

The optical transmittance I in the Clark-Lagerwall effect is calculated as follows [1–3]:

$$I = \sin^2 4\theta \sin^2 \Delta\Phi/2 \qquad (3)$$

where $\Delta\Phi = \pi\Delta nd/\lambda$ the phase difference, $\Delta n = n_\parallel - n_\perp$. As follows from (3), the maximum contrast is obtained for $\theta = \pi/8$ (22.5°), $\Delta nd/\lambda = 1/2$, which, for $\Delta n = 0.125$, $\lambda = 0.5$ μm, gives $d \approx 2$ μm. We should note, that the variation of the cell thickness $\Delta d = \lambda/8\Delta n$ from the optimum value $d = \lambda/2\Delta n$ results in a considerable difference in the FLC electrooptical response (Fig. 2) [3]. The practical criteria of an FLC display quality, however, require more precise limitations $d = 2 \pm 0.2$, μm.

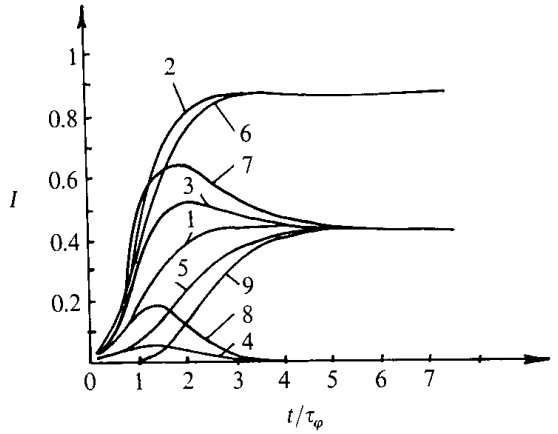

Fig. 2. Electrooptical response of the FLC cell in Clark-Lagerwall effect for different phase factors $d\Delta n/\lambda = k/4$, k= 1…9 [3]

3. Bistable and Multistable switching in FLC cells

The bistable switching in SSFLC geometry (Fig. 1) takes place above a certain threshold field $E_{th} \propto W_d/K^{1/2}$, where K is an average elastic constant and W_d is a dispersion anchoring energy and polar anchoring energy is taken equal to zero $W_p = 0$ [3]. Thus with increasing anchoring we have to increase the switching amplitude of the electric field. As the energy of switching electric torque is proportonal to the product of PE, the bistability threshold is inversely proportional to the value of the FLC spontaneous polarization P.

The problems we meet using the Clark–Lagerwall effect include not only severe restrictions to the optimum layer thickness and requirements of defectless samples, but also difficulties in the realization of a perfect bistability or optical memory switched by the electric field and also providing the grey scale. The latter problem is one of the most crucial, because it is very inconvenient to provide the grey scale using either complicated driving circuits or increasing the number of working elements (pixels) in an FLC display [1–3]. This problem arises in the Clark–Lagerwall effect because the level of transmission is not defined by the amplitude of the driving voltage pulse U, but by the product $U\tau$, where τ is the electric pulse duration.

A surface-stabilized FLC (SSFLC) structure with bistable switching cannot provide an intrinsic continuous gray scale, unless a time- or space-averaging process is applied [1–3]. The inherent physical gray scale of passively addressed FLC cells can be obtained if the FLC possesses multistable electro-optical switching with a sequence of ferroelectric domains, which appear if the spontaneous polarization *Ps* is high enough [4]. Ferroelectric domains in a helix-free FLC form a quasi-periodic structure with a variable optical density as it appears between crossed polarizers [5] (Fig. 3). The bookshelf configuration (Fig. 1) of smectic layers is preferable for the observation of these domains. If the duration of the electric pulse applied to a helix free SSFLC layer containing ferroelectric domains is shorter than the total FLC switching time, the textures shown in Fig. 3 are memorized after switching off this pulse and short-circuiting of the FLC cell electrodes. The domains appear as a quasi-regular structure of bright and dark stripes parallel to the smectic-layer planes. The bright stripes indicate the spatial regions with a complete switching of the FLC director, while the dark stripes indicate the regions that remain in the initial state. The sharp boundaries between the black and white domain stripes seem to illustrate the fact that only two stable director orientations exist. The variation of the occupied area between bright and dark stripes depends on the energy of the applied driving pulses. The total light transmission of the structure is the result of a spatial averaging over the aperture of the light passed through the FLC cell and is always much larger than the period of the ferroelectric domains. Both the amplitude and the duration of the driving pulses can be varied to change the switching energy, which defines the memorized level of FLC-cell transmission in a multistable electro-optical response. Therefore, any level of the FLC-cell transmission, intermediate between the maximum and the minimum transmissions, can be memorized after switching off the voltage pulses and short-circuiting of the cell electrodes (Fig. 3).

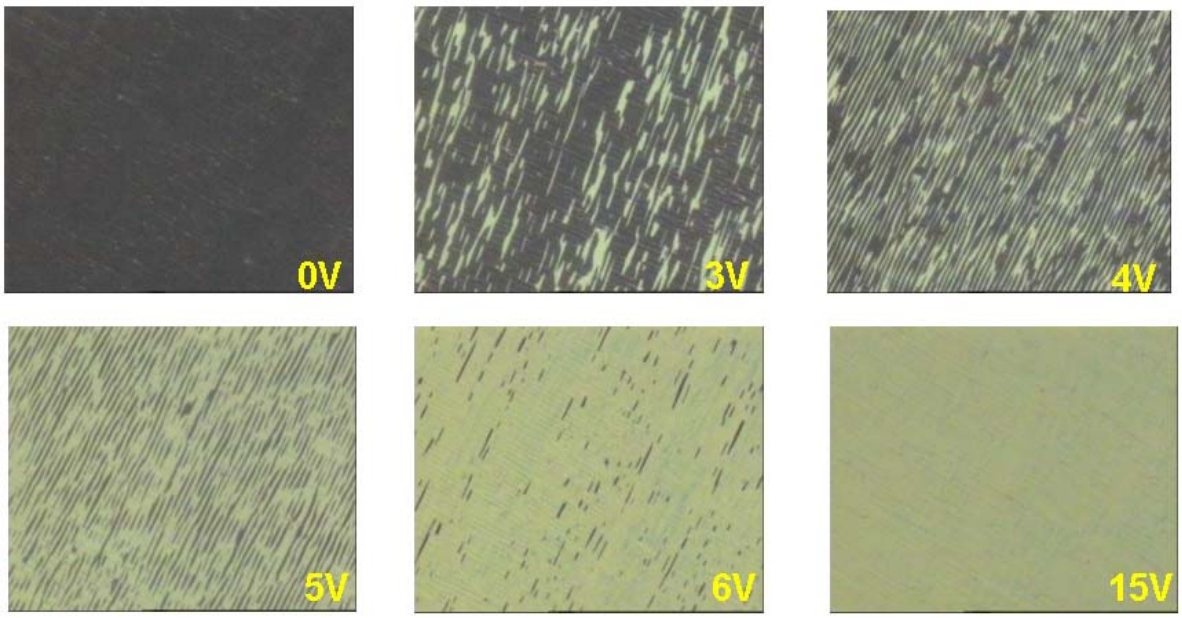

Fig. 3. Continuous variation of the width of ferroelectric domains with a change in the applied voltage of the FLC layer between crossed polarizers [5]

The necessary conditions of multistable switching modes, are (i) sufficiently high FLC spontaneous polarization Ps > 50 nC/cm^2 and (ii) a relatively low energy of the boundaries between the two FLC states existing in FLC domains (Fig. 3), which is usually typical for the antiferrroelectric phase [1–3]. The multistability is responsible for three new electro-optical modes with different shapes of the gray-scale curve that can be either S-shaped (double or single dependent upon the applied-voltage pulse sequence and boundary conditions) or V-shaped dependent upon boundary conditions and FLC cell parameters (Fig. 4).

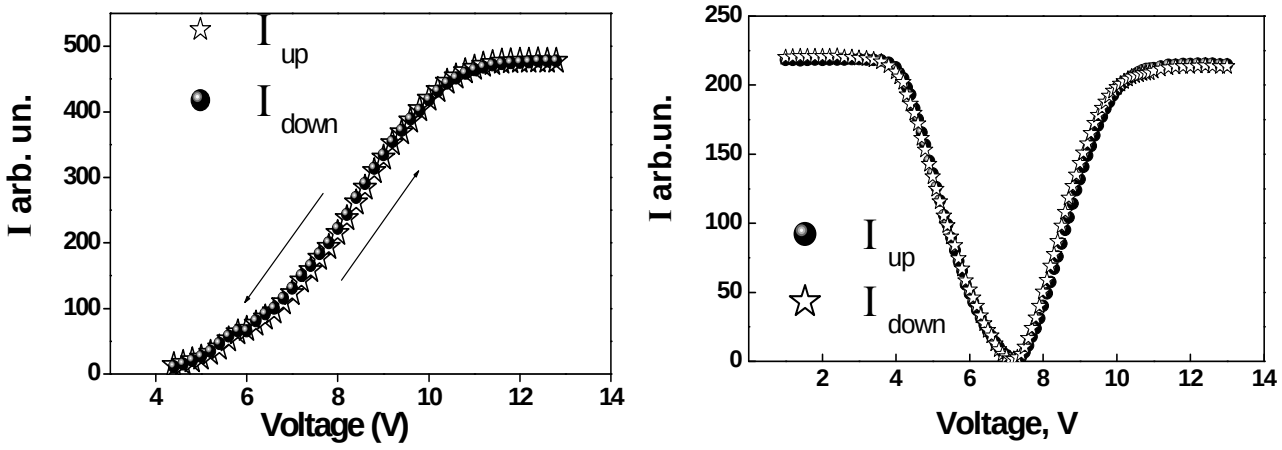

Fig. 4. S-shaped (above) and V-shape (below) FLC multi-stable switching [4]

The theoretical and experimental investigation of reversible and memorized S and V-shaped multistable FLC electro-optical modes was proposed in Ref. [4]. New electro-optical modes are based on the multistable electro-optical modes in FLC cell [4, 5] (Fig. 3).

4. Deformed Helix Ferroelectric Effect

The geometry of the FLC cell with a DHF effect is presented in Fig. 5 [6]. The polarizer (P) on the first substrate makes an angle with the helix axis and the analyzer (A) is crossed with the polarizer.

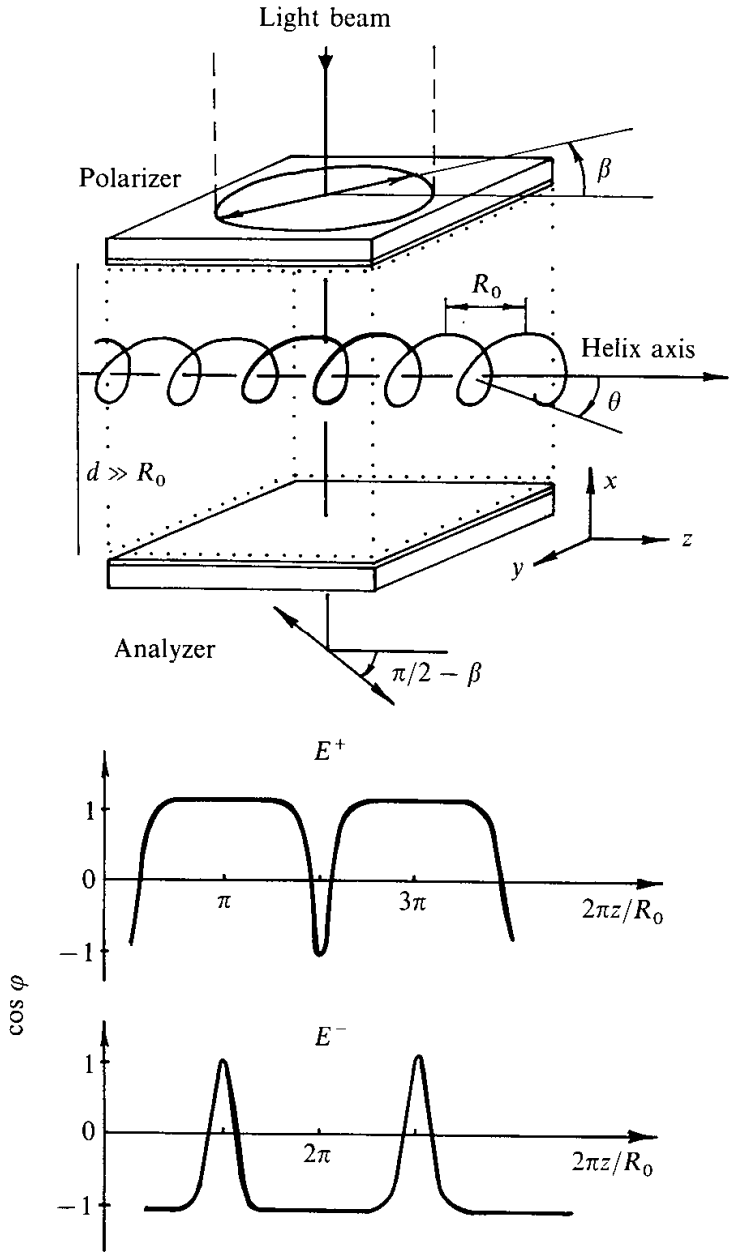

Fig. 5. Deformed Helix Ferroelectric (DHF) Effect [3]

The FLC layers are perpendicular to the substrates and the layer thickness d is much higher than the value of the helix pitch R_o:

$$d >> R_o. \quad (4)$$

The light beam with the aperture a >> R_o passes parallel to the FLC layers through an FLC cell placed between the polarizer and analyzer. In an electrical field the FLC helical structure becomes deformed, so that the corresponding dependence of the director distribution cosφ, as a function of coordinate $2\pi z/R_o$, oscillates symmetrically in ±E electric fields [3] (Fig. 5). These oscillations result in a variation of the effective refractive index, i.e., electrically controlled birefringence appears.

The effect takes place up to the fields of FLC helix unwinding [3]

$$E_U = \pi^2/16\ K_{22}q_0^2/P_s, \quad (5)$$

where K_{22} is FLC twist elastic constant, $q_0 = 2\pi/R_0$ – helix wave vector.

The characteristic response times τ_c of the effect in small fields $E/E_u << 1$ are independent of the FLC polarization P_s and the field E, and defined only by the rotational viscosity γ_φ , and the helix pitch R_o:

$$\tau_c = \gamma_\varphi/K_{22}q_0^2 \quad (6)$$

The dependence (6) is valid, however, only for very small fields E. If $E \leq E_u$, the FLC helix becomes strongly deformed and $\tau_c \propto E^{-\delta}$, where $0 < \delta < 1$ [7]. If E is close to the unwinding field E_u the helical pitch R sharply increases R >> R_o. Consequently, the times of the helix relaxation τ_d to the initial state also rise

$$\tau_d/\tau_c \propto R^2/R_0^2 \quad (7)$$

i.e., for $E \approx E_u$ it is possible to observe the memory state of the FLC structure [6]. In this regime the electrooptical switching in the DHF effect reveals a pronounced hysteresis especially for $E \Rightarrow E_u$.

However, if the FLC helix is not deformed too much, fast and reversible switching in the DHF mode could be obtained [3]. The switching time, less than 10 μs at the controlling voltage of ±20V can be provided, which is temperature independent over the broad temperature range [8]. The fast ferroelectric LC cells (deformed helix ferroelectric-DHF effect) with the response time around one microsecond in a broad temperature range from 20 to 80 degrees were developed [9] (Fig. 6). We believe, that DHF FLC are the fastest electrooptical mode in LC cells for photonics and display applications.

Fig. 6. A copy of an oscilloscope screen is presented here. The upper curve shows the driving voltage waveform (whose amplitude is ±15 Volt and frequency is 50 kHz) applied to the FLC-587 based cell with the FLC layer thickness 3μm. The bottom waveform shows the electro-optical response of the cell at T = 22 °C, λ = 0.628 μm [9]

The optical transmission of the DHF cell could be calculated as follows:

$$I = \sin^2(\pi\Delta n(z)d/\lambda)\sin^2(2(\beta-\alpha(z)), \quad (8)$$

where β is the angle between the z-axis and the polarizer (Fig. 5),

$$a(z) = \arctan(\tan\theta\cos\varphi(z)) \quad (9)$$

is the angle between the projection of the optical axis on the y, z-polarizer plane and the z-axis, and $\Delta n(z) = n_{eff}(z) - n_\perp$ is the effective birefringence:

$$n_{eff} = n_\parallel n_\perp/[\,n_\perp^2 + (n_\parallel^2 - n_\perp^2)\sin^2\theta\sin^2\varphi]^{1/2} \quad (10)$$

(Diffraction of light on the helical structure is avoided, because the helical pitch of the FLC mixture $R_o \propto 0.1$–$0.3\ \mu m < \lambda = 0.5\ \mu m$ is in the visible range).

In the case of small angles $|\theta| << 1$, the transmission in (8) can be expanded in θ series

$$I \propto (\sin^2 2\beta - 2\theta\sin 4\beta\cos\varphi + 4\theta^2\cos 4\beta\cos^2\varphi)\sin^2\pi\Delta nd/\lambda \quad (11)$$

As shown in [3] for the small values of the applied field $\cos\varphi \propto E/E_u$ and changes its sign for the field reversal $E \Rightarrow -E$ (Fig. 5). Thus according to (11) for $\sin 4\beta = 0$ we have a quadratic grey scale, i.e.

$$\Delta I \propto \theta^2\cos^2\varphi \propto \theta^2\ E^2/E_u^2 \quad (12)$$

and for other values of θ the grey scale is linear. For $\cos 4\beta = 0$ the quadratic component in the modulated intensity I is absent , i.e.

$$\Delta I \propto \theta\cos\varphi \propto \theta\ E/E_u \quad (13)$$

If $E(t) = E_o \cos\omega t$, then in the case of (12) we come to the modulation regime, which doubles the frequency

of the applied field. The relationships (12), (13) were confirmed in experiment [6]. Using a «natural» grey scale of the DHF mode many grey levels have been obtained with fast switching between them [10]. New ferroelectric mixtures with the helix pitch $R_0 < 0.3$ μm um and tilt angle 0 > 30° have recently been developed for the DHF effect [10, 11]. The helix unwinding voltage was about 2–3 V. Short-pitch FLC mixtures could be also used to obtain pseudo-bistable switching in FLC samples. Using these new FLC's, the electrically controlled V-shaped switching in DHF mode can be applied for new active-matrix LCD with Field Sequential Colors (FSC) [3].

A geometry with β = 0 was selected in all experiments to provide non-sensitive to the driving voltage polarity electro-optical response. Maximal light transmission under this condition, as it follows from (8), occurs if α(z) =45° and Δn(z)d = λ/2. It is easy to show from (8) that the tilt angle θ of the FLC should be close to 45° for providing of maximal light transmission at β = 0. The typical V-shape symmetrical (voltage sign independent) DHF switching is shown in Fig. 7 [10].

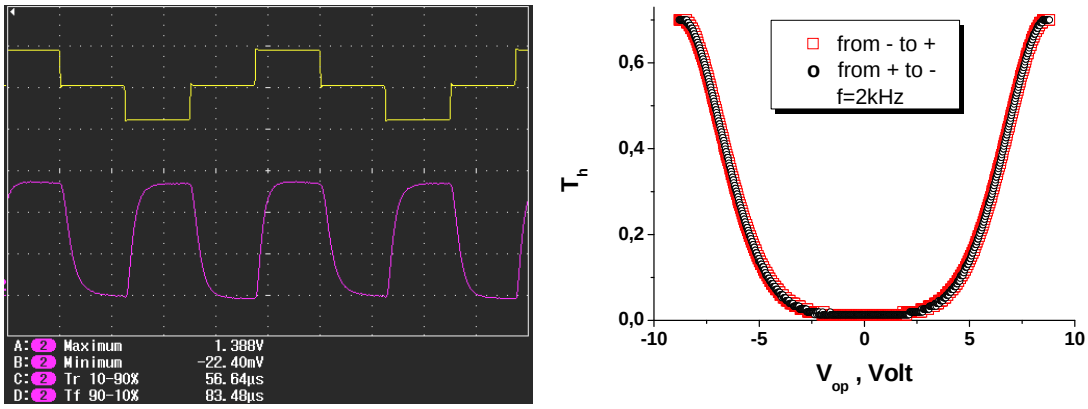

Fig. 7. Symmetric (voltage sign independent) electrooptic response of DHF – FLC [10]. Left: Top – the driving voltage waveform applied to the cell, bottom – the electro-optical response of the cell. Right: V-shaped mode in the envelope curve of light transmission saturation states measured at electro-optical response frequency 2 kHz. The light transmission T_h evaluated in comparison with transmission of empty cell placed between parallel polarizers; this transmission is defined as $T_h = 1$

Let us point to certain advantages of the DHF electrooptical effect for applications as compared with the Clark–Lagerwall mode.

1. High operation speed is achieved for low driving voltages. This takes place because a slight distortion of the helix near the equilibrium state results in a considerable change in the transmission. Consequently, the instantaneous response of the FLC cell is provided without the so-called delay time inherent to the Clark–Lagerwall effect.

2. The DHF effect is also less sensitive to the surface treatment and more tolerant to the cell gap inhomogeneity. As follows from experiment and qualitative estimations [3] the effective birefringence value Δn_{eff} is approximately twice as low as $\Delta n = n_{\parallel} - n_{\perp}$ in the Clark–Lagerwall effect.

3. The DHF effect allows the implementation of a «natural», i.e., dependent on voltage amplitude, grey scale both linear and quadratic in voltage. Moreover, at $E \approx E_u$ long-term optical memory states are possible. In particular, a high quality dark state of DHF FLCD has been obtained as well as V-shape switching with a high frequency [12] (Fig. 7). Two inherent properties of DHF-FLC have been observed (Fig. 7): (i) similar to NLC cells, the electro-optical response is insensitive to the driving voltage polarity, but the response time is two orders faster as compared with NLC, i.e. $\tau^{on}_{0.1-0.9} \cong 80\ \mu s$, $\tau^{off}_{0.1-0.9} \cong 60\ \mu s$; (ii) the response exhibits perfect V-shaped mode obtained for the case of rectangular alternating applied voltage pulses shown in Fig. 7. As is illustrated in Fig. 7, the electro-optical response frequency is twice higher than the driving voltage frequency. The cell was controlled by the voltage waveform appropriate for FSC displays. Figure 7 shows that the cell light transmission is continuously tunable for each color field independently at both voltage polarities.

Thus V-shaped electro-optical response is shown to be an inherent property of a DHFLC cell under

a special choice of the applied rectangular alternating electric field waveform, frequency, and the cell geometry. In contrast to other known V-shaped FLC modes, the discovered V-shaped switching is observed in a broadband frequency range including one kilohertz, and not at a certain characteristic frequency. Frequency independent V-shaped DHFLC switching allows increasing drastically (up to 1 kHz) the operating frequency of FSC LCD cells.

A special software for an advanced design of new FLCD prototypes [13, 14]. Certain new FLCD prototypes can be optimized using our software, including the optimization of FLC configuration as well as the optical scheme. One of remarkable properties of DHF mode is independence of the response time on applied voltage at V < Vc. Another characteristic feature of DHF mode is frequency dependence of the electro-optical response time, which is really exists in our case shown in Fig. 8. We have found that the switching time of DHF FLC decreases with frequency of the applied voltage, which is in a good agreement with our experimental results [15] (Fig. 8).

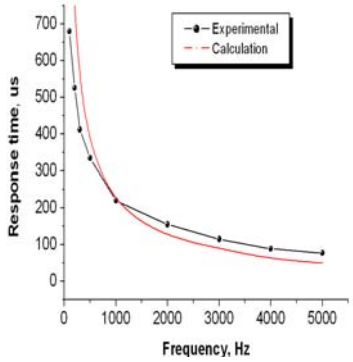

Fig. 8. Response time of DHF FLC as a function of the applied voltage frequency [15]

5. Electrically suppressed helix (ESH) mode

A new electrooptic mode, found recently was called Electrically Suppressed Helix (ESH) mode [12, 16]. The mode is characterized by a high contrast ratio and very fast electrooptic response and is highly suitable for display and photonics applications. Deformed helix ferroelectric (DHF) mode exists at $V \leq V_c$ = 0.4V and the helix is completely suppressed by electric field at V ≥ 1V, see Fig. 9 right part and linear dependence of the inverse response time at V > 1V in Fig. 10, where the response time has absolutely the same behavior as in SSFLC mode. Despite of these similarities, it should be emphasized that at V > V_c, strictly speaking, there is no SSFLC mode but an electro-optical mode with completely electrically suppressed helix arises (ESH-mode). It would seem that between SSFLC and ESH modes there is only a formal difference in initial conditions (the helix is suppressed by surfaces in SSFLC, but this does not happen with ESH), as the dynamics of a completely identical. Actually, the presence of helix without applied voltage is the cause of the unique high alignment quality in ESH-mode (see top right insertions in Fig. 9). The contrast ratio in ESH mode is more than 12000:1 up to 1 kHz at ±1.5V and up to 2 kHz at ±3V; the light transmission is about of maximum in this case, see insertion to Fig. 11.

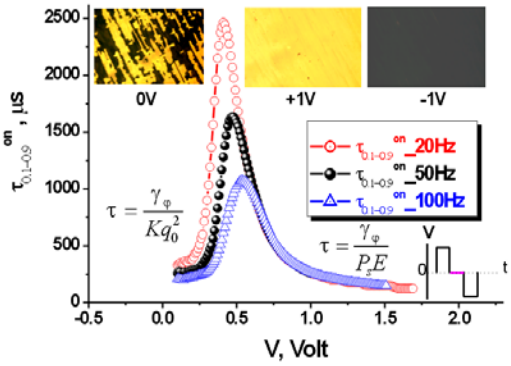

Fig. 9. Dependence of switching on time of 1.5 μm cell filled with the FLC-595 [12, 16]. Insertions: bottom right is the driving voltage waveform; top the FLC layer textures between crossed polarizers, horizontal scale of all images is 200 μm; top left – the voltage is not applied, top right – textures at +1V and –1V

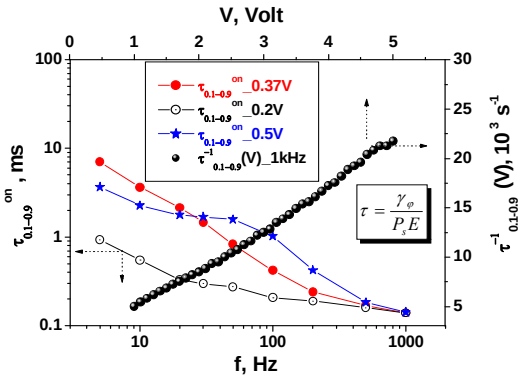

Fig. 10. The frequency dependencies of the response time at different voltages under condition V ≤ 0.5V; (•) – linear dependence of the inverse response time $\tau^{-1}_{0.1-0.9}(V)$ at V > 1V [12, 16]

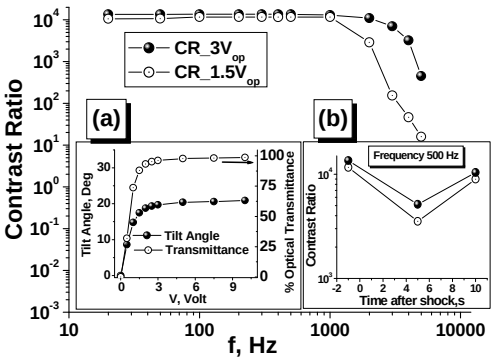

Fig. 11. Dependencies of the contrast ratio on driving voltage frequency at V=1.5V and V=3V. The FLC-595 [12, 16] layer thickness is 1.5 μm, no SiO_2 layers, measurements have been carried out at T = 22°C, wavelength λ = 0.63 μm. Insertion left: Dependencies on voltage: measured tilt angle and the cell light transmission in comparison with transmission of empty cell placed between crossed polarizers. Insertion right: Contrast ratio dependence on time after the application of mechanical shock

The unique high alignment quality, however, is observed only if the helix elastic energy is comparable but obligatory not less than the anchoring energy normalized to d_{FLC}:

$$Kq_0^2 \geq \frac{2W_Q^0}{d_{FLC}}, \qquad (14)$$

where W_Q^0 is a coefficient the anchoring energy. We have measured $W_Q^0 = 4 \cdot 10^{-4}$ J/m^2 just for the cell whose properties are illustrated in Figs. 9, 10, thus confirming the validity of inequality (14), when outstanding alignment quality (top right insertions in Fig. 9) is observed.

A very uniform FLC alignment exists just only in ESH-mode when $V > V_c$ (right top insertion in Fig. 9) while at $V < V_c$ it is worse because the FLC layer is divided into two-domain helical structures with the domains principal axes deployed at an angle around double FLC tilt angle 2θ. When observed with a polarizing microscope, these helical domains are perceived as homogeneous dark and light areas with their characteristic sizes around 10–50 μm, see left top insertion in Fig. 9. The domains are completely suppressed by a weak electric field $E_c < E < 1$V/μm (right top insertion in Fig. 9) thus forming perfect chevron-free alignment in ESH-mode.

In addition to this the shock stability has also been found good for the ESH mode. The contrast ratio was measured with time after removing the mechanical pressure. The contrast can be restored in very short time after removal of mechanical pressure (Fig. 11). The electro-optical response manifests evident saturation at 500 Hz and ±1.5V with the response time $\tau_{0.1-0.9}$ = 130 μs (Figs. 9, 10).

6. Orientational «Kerr effect» in DHF FLC with subwavelength pitch

The Kerr like non-linearity has been observed in ferroelectric liquid crystals (FLC) with sub-wavelength helix pitch [17, 18]. In order to systematically examine the pure phase modulation of light that takes place when the selective reflection from the helix is suppressed, FLC with the helix pitch R=p_0 = 150 nm was used. Vertical alignment of the FLC with the well-known geometry of inter-digital electrodes have been used to orient the helix axis perpendicular to the substrates while electric field is parallel to smectic layers. In the absence of electric field, the FLC helical structure was optically equivalent to a uniaxial crystal whose principle axis coincides with the axis of the helix. Whereas, in the presence of electric field E, the in-plane refractive indices along ($n_{//}$) and perpendicular ($n_{\perp}$) to the field differ from each other and their difference is proportional to square of the field: $\delta n_{ind} \propto E^2$. Thus, proposed phase modulator exhibits hysteresis free 2π phase modulation with constant ellipticity of emerging light and response time less than 100 μs, thus it could find application in many modern electro-optical devices.

Figure 12, (*a)* presents the extensive overview of the electro-optical cell with standing FLC helix and inter-digital electrode deployed on one of the two glass plates [18]. The inter-digital electrodes with electrode width 2 μm and electrode gap of 50 μm have been deployed to apply electric field parallel to the smectic layers. The vertical alignment to the DHF FLC has been accomplished by spin coating glass plates with 40 nm thick layer of stearic acid chromium salt (Fig. 12, *a*) followed by soft backing at 100 ºC for 10 min. The Fig. 12, (*c)* represents the optical micro-photograph of the a vertically aligned DHF FLC (VADHFLC) cell under crossed polarizers and in the absence of the electric field.

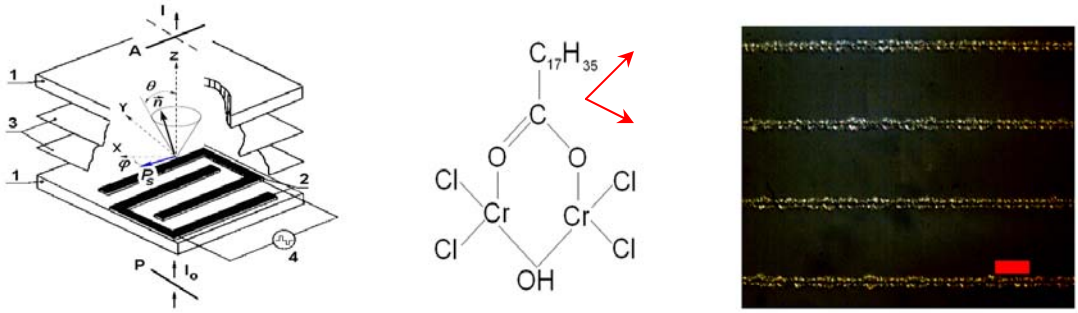

a *b* *c*

Fig. 12. a – Schematic representation of geometry of a vertically aligned DHFLC cell [18]: 1 are glassy plates, 2 are in-plane electrodes, 3 are smectic layers parallel to glassy substrates, 4 is a voltage generator, P (A) is polarizer (analyzer), θ is the tilt angle of director $\boldsymbol{n}$ in smectic layers, φ is azimuthal angle of the spontaneous polarization vector $\boldsymbol{P_s}$, I_0 is intensity of incident light, I is intensity of light transmitted through the ADHFLC cell placed between P and A; *b* – the chemical structure of stearic acid chromium salt; *c* – the micro-photograph of VADHFLC cell placed between crossed polarizers at V = 0. The red mark is equal to the 20 μm

Figure 13, (*a*) reveals the schematic diagram of the VADHFLC cell where the DHFLC principal axis (PA) and its interaction with the applied electric field [18]. In the presence of electric field E, (i.e. < E_c), the PA deviates from its initial position z by an angle $\Delta\alpha$ in a plane perpendicular to the electric field direction and as a consequence the refractive indices of the helical structure along ($n_{E_{II}}$) and perpendicular ($n_{E_\perp}$) to the electric field (Fig. 13, *b*) differ from each other and their difference corresponds to the biaxiality (δn_{ind}) of the helical structure.

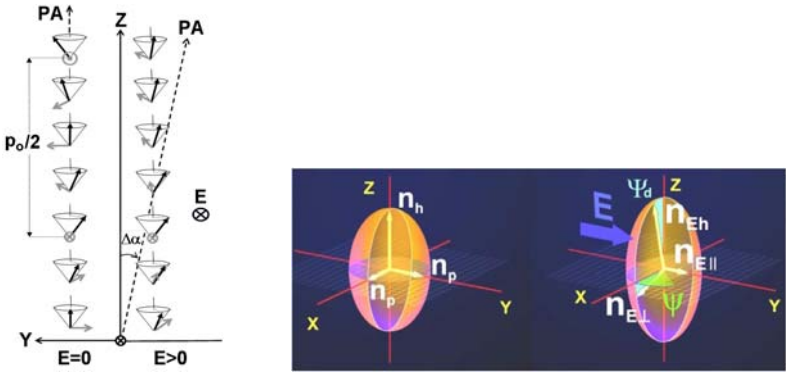

a *b*

Fig. 13. a – illustration of the VADHFLC principal axis deflection in the presence of electric field, *b* – schematic representation of the refractive indices ellipsoid in the absence (left) and in the presence (right) of electric field [18]

For normally incident light, the electrically controlled birefringence writes [17, 18]:

$$\delta n_{ind} = n_{\|E} - n_{\perp E} = K_{Kerr} E^2, \qquad (15)$$

where $n_{\|E}$ and $n_{\perp E}$ the effective DHF FLC refractive indexes, induced parallel and perpendicular to the appluied electric field and «Kerr constant»

$$K_{Kerr} = 2\, n_{E=0} \cdot (1 - n^2_\perp / n^2_{E=0}) \cdot (\chi_E / P_s)^2 \qquad (16)$$

is proportional to the «isotropic» refractive index for zero electric field $\alpha_{Kerr} \sim n_{E=0}$, shown below:

$$n^2_{E=0} = [n^2_{\|}\, n^2_{\perp} / (n^2_\perp + (n^2_{\|} - n^2_\perp)\cos^2\theta)^{1/2} + n^2_\perp]/2,$$

$n_{\|}$ and $n_\perp$ FLC refractive indexes and θ – FLC tilt angle, P_s–FLC spontaneous polarization, and $\chi_E = \partial P_s < \cos\varphi > / \partial E$ – FLC average dielectric susceptibility along the field direction.

The FLC transmittance T as a function of the E^2 is shown in Fig. 14. This figure reveals that the VADHFLC cell shows the 2π phase modulation at the electric field of ~ 2.1 V/μm. The light transmission of VADHFLC cell between two crossed polarized can be described by [17, 18]:

$$T = \sin^2 2\Psi \sin^2 \frac{\pi \delta n_{ind} d_{FLC}}{\lambda} , \qquad (17)$$

where d_{FLC} corresponds to the FLC layer thickness. Thus, the δn_{ind} has been computed from Eqs. (15) and plotted in Fig. 14. The open circular legends in Fig. 14 represent the experimental data while the solid blue line represents the theoretical fit of Eqs. (15). The value of δn_{ind} for FLC-587 at saturation is 0.05, which means that 2π modulation can be obtained for the FLC thickness to wavelength ratio d_{FLC}/λ = 20 (Fig. 14). This is a reasonable thickness of FLC cell, which will still keep the high quality FLC orientation even for IR light [17, 18].

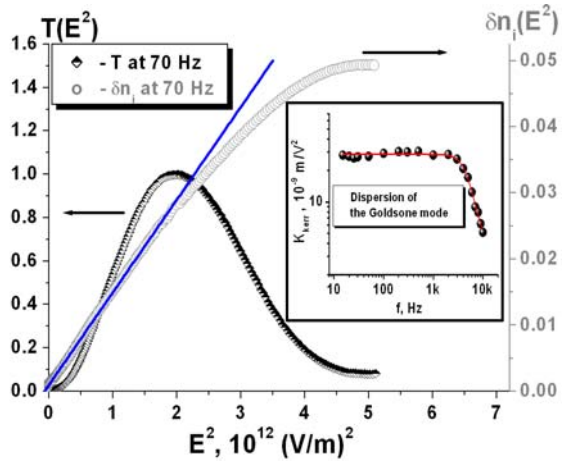

Fig. 14. The transmittance $T(E^2)$ (♦) and $\delta n_{ind}(E^2)$ (○) dependence for VADHFLC cell placed between crossed P and A at Ψ = 45°at the applied frequency of 70 Hz [18]. The solid blue line is the result of theoretical fit of the δn_{ind} according to eq. (15). Insertion: shows the plot of Kerr constant «*K*» with frequency and solid red line represent the theoretical fit

With the help of experimental results for δn_{ind} and eq. 15, K_{kerr} has been evaluated at different frequencies and plotted in the insertion of Fig 14. The K_{kerr} = 27 nm/V^2, which is about four orders of magnitude greater than the Kerr constant of nitrobenzene and twice larger than the Kerr constant of the best known polymer stabilized blue phase LC (PSBPLC) [19]. The K_{kerr} is constant till the frequency of 2 kHz afterwards, at higher frequencies, it shows clear dispersion. This dispersion can also be explained on the basis of eq. 15. The K_{kerr} depends on the dielectric susceptibility of the goldstone mode (χ_E) that is defined as [17, 18]:

$$\chi_E = \frac{P_s^2}{2Kq_0^2} , \qquad (18)$$

where *K* is the elastic constant while the $q_o = 2\pi/R_0$ is the wave vector of the helix, thus K_{kerr} can be increased further by optimizing the FLC material parameters.

The phase modulation of light in FLC orientational «Kerr effect» occurs only because of the electrically induced variation of the FLC refractive indices. Consequently, no modulation in the ellipticity of output light has been observed (Fig. 15). For $E < E_c$, the ellipticity is independent on the electric field which is the same range of the electric field where the δn_{ind} remains quadratic. However, near E_c and at higher electric field the $\delta n_{ind}(E)$ deviates from the quadratic dependence on *E* and simultaneously the ellipticity of the emerging light begins to increase. This increase in the ellipticity is because of the helix unwinding process near E_c that results in polarization plane rotation of impinging light.

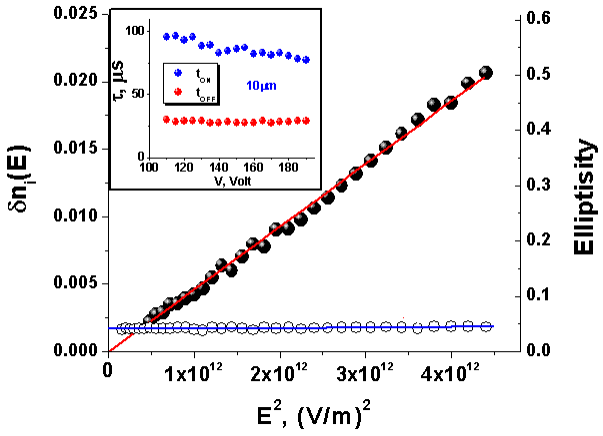

Fig. 15. Solid legends represents the δn_{ind} of 18 μm thick vertically aligned DHFLC cell and open legends are for the ellipticity of the emerging light at the frequency of 40 Hz [18]. The insertion represents variation of the t_{ON} and t_{OFF} with respect to the applied voltage

The insertion in Fig. 15 represents the electric filed dependence of the t_{ON} and t_{OFF}. The VADHFLC device is characterized by the fast response time less than 100 μs and thus the modulation frequency could as high as 1 kHz with saturated electro-optical states.

In recent time PSBPLC has been considered as emerging display and phase modulating technology however, the VADHFLC seems more appropriate because of higher Kerr constant, hysteresis free electro-optics and faster (around an order of magnitude) electro optical response. Thus, VADHFLC could find application in many modern electro-optical devices.

7. Conclusion

Fast response time, high contrast ratio various FLC electrooptical modes, such as Clark-Lagerwall mode is Surface Stabilized FLC (SSFLC) structure, Bi and Multistable FLC switching, Deformed Helix Ferroelectric (DHF), Electrically Suppressed Helix (ESH) mode, and FLC orientational electro-optic Kerr effect were proposed for fast FLCD are achieved through the application of photoaligning layers in FLC cells. Fast FLCD with a high resolution can be used in the screens field sequential color (FSC) FLC microdisplays, which are now one of the most advanced technologies for pico-projectors. The switchable goggles and lenses based on new FLC prototypes can be efficiently applied in the new generation of switchable 2D/3D LCD TVs. The further development of novel fast ferroelectric LCD aimed at (i) development of new fast responded FLC materials with fast switching and a sufficient number of switchable gray levels (V-shape switching); (ii) implementation of the working prototypes of novel field sequential color (FSC) FLC displays, including the 3D version [12]; (iii) investigations of regimes of operation to allow to use efficient addressing of FLCD including TFT drivers enabling a high switching current; (iv) solving the problem of a mechanical stability of FLC layers; (v) mass production of new FLC materials with optimal characteristics.

References

1. Clark N.A., Lagerwall S.T. Submicrosecond bistable electrooptic switching in liquid crystals. *Appl. Phys. Lett.,* 1980, **36** (11), 899–901.
2. Lagerwall S.T. Ferroelectric and antiferroelectric liquid crystals. *Ferroelectrics*, 2004, **301** (1), 15–45.
3. Chigrinov V.G. Liquid Crystal Devices: Physics and Applications. Artech-House, Boston-London, 1999. 366 p.
4. Pozhidaev Evgeniy, Chigrinov Vladimir, Hegde Gurumurthy, Xu Peizhi. Multistable electro-optical modes in ferroelectric liquid crystals. *J. SID*, 2009, **17** (1), 53–59.
5. Pozhidaev E P., Chigrinov V.G. Bistable and Multistable States in Ferroelectric Liquid Crystals. *Crystallography Reports,* 2006, **51** (6), 1030–1040. **DOI**: 10.1134/S1063774506060149
6. Beresnev L.A., Chigrinov V.G., Dergachev D.I., Pozhidaev E.P., Funfschilling J., Schadt M. Deformed helix ferroelectric liquid crystal display: a new electro-optic mode in ferroelectric chiral smectic C liquid crystal. *Liq. Cryst.,* 1989, **5** (4), 1171–1177.
7. Panarin Yu., Pozhidaev E., Chigrinov V. Dynamics of controlled birefringence in an electric fielf deformed helical structure of a ferroelectric liquid crystal. *Ferroelectrics*, 1991, **114**, 181–186.
8. Pozhidaev E.P. Electrooptical properties of deformed-helix ferroelectric liquid crystal display cells. *Proc. of SPIE: Advanced Display Technologies,* 2001, **4511**, 92–99.
9. Pozhidaev E.P., Molkin V.E., Chigrinov V.G. Smectic nanostructures with a typical size less than a visible light wavelength: physics and electro-optics. *Photon. Letts. of Poland*, 2011, **3**, 11–13.
10. Pozhidaev Evgeny, Chigrinov Vladimir. Fast Photo-Aligned V-shape Ferroelectric LCD Based on DHF Mode. *SID'10 Digest*, USA, Seattle, 2010, 387–390.
11. Gurumurthy Hegde, Peizhi Xu, Pozhidaev Eugene, Chigrinov Vladimir, Hoi Sing Kwok. Electrically controlled birefringence colours in deformed helix ferroelectric liquid crystals. *Liq. Cryst*., 2008, **35** (9), 1137–1144.
12. Chigrinov V.G., Hoi-Sing Kwok. Photoalignment of liquid crystals: applications to fast response ferro-electric liquid crystals and rewritable photonic devices. *Progress in Liquid Crystal Science and Technology: in Honor of Shunsuke Kobayashi's 80th Birthday*, Singapore: World Scientific, 2013, **4** (8).
13. Yakovlev Dmitry, Chigrinov Vladimir, Hoi Sing Kwok, *to be published*.
14. Kiselev A.D., Pozhidaev E.P., Chigrinov V.G., Hoi-Sing Kwok. Polarization-gratings approach to deformed-helix ferroelectric liquid crystals with subwavelength pitch. *Phys. Rev. E*., 2011, **83**, 031703 (1–11).
15. Chigrinov Vladimir, Pozhidaev Eugene, Srivastava Abhishek, Qi Guo, Fan Fan, Ma Ying, Lastochkin Anton, Kwok Hoi Sing. Novel Photoaligned Fast Ferroelectric Liquid Crystal Display. *18 Intern. Display Workshop.* Nagoya, Japan, 2011, 557–560.
16. Pozhidaev E.P., Minchenko M., Molkin V., Torgova S., Srivastava A.K., Chigrinov V., Kwok H.S., Vashenko V., Krivoshey A. High Frequency Low Voltage Shock-Free Ferroelectric Liquid Crystal: A New Electro-Optical Mode with Electrically Suppressed Helix. *Intern. Display Research Conference EuroDisplay* 2011. Arcachon, France, September, 2011. Oral 1.3.
17. Pozhidaev E.P., Kiselev A.D., Chigrinov V.G., Srivastava A.K., Minchenko M.V., Kotova S.P.

Orientational Kerr-effect in Ferroelectric Liquid Crystals. *Abstracts of 24-th Intern. Liq. Cryst. Conf. ILCC-2012,* Germany, Mainz, August 2012, Abstract 5551_0208.

18. Pozhidaev E.P., Kiselev A.D., Srivastava Abhishek Kumar, Chigrinov V.G., Kwok Hoi-Sing, Minchenko M.V. Orientational Kerr effect and phase modulation of light in deformed-helix ferroelectric liquid crystals with subwavelength pitch. *Phys. Rev. E.*, 2013, **87**, 052502 (1–8).
19. Rao L., Yan J., Wu S.T., Yamamoto S., Haseba Y. A large Kerr constant polymer-stabilized blue phase liquid crystals. *Appl. Phys. Lett.*, 2011, **98** (8), 081109.

Поступила в редакцию 2.09.2015 г.
Received 2 September, 2015